ACS OMEGA

http://pubs.acs.org/journal/acsodf

Article

Amphiphilic Chitosan Bearing Double Palmitoyl Chains and Quaternary Ammonium Moieties as a Nanocarrier for Plasmid DNA

Thev Pol, Wunpen Chonkaew, Lalintip Hocharoen, Nakorn Niamnont, Namphueng Butkhot, Yaowaluck Maprang Roshorm, Suda Kiatkamjornwong, Voravee P. Hoven, and Kornkanya Pratumyot*

Cite This: *ACS Omega* 2022, 7, 10056−10068

Read Online

ACCESS | Metrics & More | Article Recommendations | Supporting Information

ABSTRACT: Amphiphilic chitosan, bPalm-CS-HTAP, having *N*-(2-((2,3-bis(palmitoyloxy)propyl)amino)-2-oxoethyl) (bPalm) groups as double hydrophobic tails and *O*-[(2-hydroxyl-3-trimethylammonium)] propyl (HTAP) groups as hydrophilic heads was synthesized and evaluated for its self-assembly properties and potential as a gene carrier. The degree of bis-palmitoyl group substitution (DS_{bPalm}) and the degree of quaternization (DQ) were approximately 2 and 56%, respectively. bPalm-CS-HTAP was found to assemble into nanosized spherical particles with a hydrodynamic diameter (D_H) of 265.5 ± 7.40 nm (PDI = 0.5) and a surface charge potential of 40.1 ± 0.04 mV. bPalm-CS-HTAP condensed the plasmid pVAX1.CoV2RBDme completely at a bPalm-CS-HTAP:pDNA ratio of 2:1. The self-assembled bPalm-CS-HTAP/pDNA complexes could enter HEK 293A and CHO cells and enabled gene expression at negligible cytotoxicity compared to commercial PEI (20 kDa). These results suggested that bPalm-CS-HTAP can be used as a promising nonviral gene carrier.

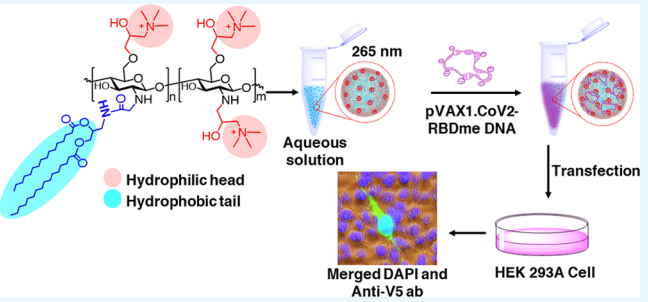

1. INTRODUCTION

Gene therapy and vaccination are methods that introduce exogenous genes in the form of plasmid DNA (pDNA) and mRNA into an individual's body; thus, a target protein is produced and functions either to replace the dysfunctional protein or to stimulate an immune response.[1−5] Due to the instability of DNA and RNA in serum media and unfavorable translocation of naked nucleic acids through the cell membrane, a carrier system is developed to bind nucleic acids, providing a protecting shell to shield the gene from serum nucleases and transport nucleic acid cargos into target cells. This process is known as transfection.[6,7] There are two major types of delivery agents: viral vectors and nonviral vectors. Although the former has been proven to possess high transfection efficacy and yield several FDA-approved drugs,[1] there have been reports on several undesirable side effects including uncontrolled cell proliferation of transduced cells, induction of vector-specific immune response, and random genomic integration.[8] The latter, on the other hand, exhibits an excellent safety profile and chemical tunability. However, they are less effective regarding gene delivery to target cells compared with viral vectors.[9] Thus, it remains a challenge among several research groups that aim to develop gene carriers with increased transfection efficiency and minimized cytotoxicity.

Cationic lipids and cationic polymers are among popular platforms for gene carriers.[10,11] Delivery of nucleic acids using lipid nanoparticles (LNPs) has reached clinical trials. Although LNPs exhibit very low immune activation,[12] they provide only a short-term genetic activity of the transported nucleic acids in cells, thus requiring continuous infusion or frequently repeated administration.[3,4,13] Cationic polymer-based delivery systems, on the other hand, provide better sustained release due to their high molecular weight, hence increasing the bioavailability of nucleic acid cargos inside cells.[14] They have been widely reported to inherently offer unlimited gene packaging capacities through electrostatic interaction and allow versatile molecular modifications. Polyethyleneimine (PEI) is one of the popular cationic polymers that possess excellent gene complexation capability and offer high transfection efficiency; however, it was reported to exhibit high toxicity on clinical trial applications.[7] The abundant positively charged PEI could form nonspecific interactions with negatively charged components of phagocytosis, resulting in large aggregates, thus inducing immune responses.[15] Several strategies have been exploited to address this dilemma of polycations such as poly(ethylene glycol) (PEG) modification of cationic polymers[16,17] and

Received: October 31, 2021
Accepted: February 3, 2022
Published: March 17, 2022

charge-reversal copolymers.[15,18,19] These strategies mask the cations from absorbing negatively charged components in the cell medium before reaching the target tissues, improving the efficiency of gene delivery. Nevertheless, none of the polycation-based gene therapy has been FDA-approved.[20] Therefore, further development of cationic polymers is necessary to achieve safe and efficient gene administration.

A natural polymer such as chitosan is a ubiquitous component of a biological system that can be harnessed to improve its function as a gene carrier. Chitosan consists of random β (1−4)-linked D-glucosamine and *N*-acetyl-D-glucosamine units, and it can be extracted from chitin present in the exoskeleton of most of the crustaceans via partial alkaline hydrolysis of acetyl groups. Chitosan has complementary properties toward gene carriers as it presents low toxicity (LD_{50} of 16 g/kg < LD_{50} of NaCl of 3 g/kg), low immunogenicity, and good biocompatibility.[4] However, its low solubility in various solvents limits its application.[21] Many investigations have been performed to tackle these limitations. For example, the hydrophilic modification with glycol,[22,23] PEG,[6,24] quaternized entities,[25−27] cyanoguanidine,[28] amino acid,[29] and polyethyleneimine[8,30−32] promotes the aqueous solubility of chitosan. In addition, lipid modifications with *N*-fatty acid,[33−38] deoxycholic acid,[39] alkyl,[40] and Brij-S20[41] drive molecular self-assembly into the core−shell structure in aqueous environments and promote the attachment of the materials to the cell membrane. Some researchers developed dual modifications such as hexanoic acid and PEG,[42] 5β-cholanic acid and PEG,[43,44] and dodecanal and carboxymethyl chitosan[45] to improve stability of the modified chitosan against the physiological environment and enhance gene transfection efficiency.[46,47] Even though the cationic lipids having shorter hydrophobic tails (C12−C14) were reported to produce a higher transfection activity than those having longer tails (C15−C18),[48,49] the amphiphilic dendrimers incorporated with longer hydrophobic tails (C18) were reported to exhibit a better transfection efficiency than those having shorter tails (C13−C15). Therefore, the influence of the hydrophobic length on transfection efficacy of gene carriers may also depend on their molecular structures and electronic properties, which affect the physical characteristics of the carriers such as self-assembly properties including the size, surface charge, morphology, and phase transition temperature. Moving to the chitosan platform, Sharma and Singh discovered that among several fatty acid-modified chitosan with various alkyl chain lengths (C6−C20), palmitic acid (C16)-modified chitosan expressed the best plasmid pGFP transfection efficacy toward HEK 293 cells.[38] To the best of our knowledge, a double installation of hydrophobic fatty acid chains onto the chitosan backbone has never been reported. Most of the LNPs successfully used for human vaccination such as Pfizer-BioNTech and Moderna Covid-19 vaccines were composed of multiple branched lipid components such as 1,2-distearoyl-*sn*-glycero-3-phosphocholine, 2-[(polyethylene glycol)-2000]-*N*,*N*-ditetradecylacetamide, and ((4-hydroxybutyl)azanediyl)-bis(hexane-6,1-diyl)bis(2-hexyldecanoate).[50] Indeed, 2-alkyl-branched lipid chains could induce the formation of lipid phases[51] that enable membrane fusion and endosomal escape, a crucial factor for successful gene delivery.[52] To exploit the structural advantage of palmitoyl groups in a double-tail lipid form that promotes cell fusion[53,54] and the inherited polymeric characteristic of chitosan that offers a high molecular weight and a biocompatible property, herein, we proposed a novel amphiphilic chitosan, bPalm-CS-HTAP, containing *N*-(2-((2,3-bis(palmitoyloxy)propyl)amino)-2-oxoethyl) (bPalm) groups as double hydrophobic tails and *O*-[(2-hydroxyl-3-trimethylammonium)] propyl (HTAP) groups as hydrophilic heads (Figure 1) as a new hybrid of high-M_W biocompatible

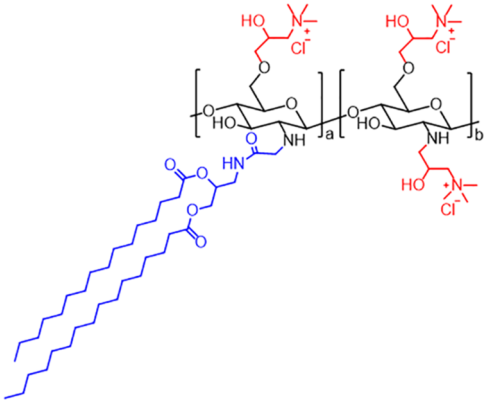

Figure 1. Chemical structure of bPalm-CS-HTAP.

chitosan and fusogenic phospholipid-like entity. This newly designed bPalm-CS-HTAP was investigated for its self-assembly as well as biological properties in order to determine its potential use in gene delivery applications. The double palmitoyl chain is biocompatible and should provide stability to the self-assembled structure. HTAP as the hydrophilic moiety with positive charges should provide binding sites for negatively charged genetic materials, yielding polyplex nanostructures.[32,55−58] bPalm-CS-HTAP particles were characterized by several techniques, including Fourier transform infrared spectroscopy (FT-IR), nuclear magnetic resonance spectroscopy (NMR), scanning electron microscopy (SEM), and dynamic light scattering (DLS) techniques. In addition, the ability of bPalm-CS-HTAP to interact with genetic materials was investigated by electrophoretic mobility shift assay (EMSA). The cytotoxicity and transfection efficiency of bPalm-CS-HTAP were tested against two cell lines, HEK 293A and CHO, using trypan blue staining and CCK-8 assay for cytotoxicity assessment and the plasmid pVAX1 harboring a gene encoding a V5-tagged chimeric protein designed from SARS-CoV-2 or pVAX1.CoV2RBDme (pDNA) as a pDNA model.

2. RESULTS AND DISCUSSION

2.1. Synthesis and Chemical Characterization of bPalm-CS-HTAP. Chemical modification of chitosan is plausible due to the reactive amino ($-NH_2$) and hydroxyl (−OH) groups at positions C2 and C6, respectively (Figure 1). Due to the more nucleophilic amino groups, we first react chitosan with the bromoacetamido unit of compound **4** via a nucleophilic substitution reaction to get *N*-(2-((2,3-bis-(palmitoyloxy)propyl)amino)-2-oxoethyl) (bPalm) groups attached at the C2 position of chitosan, yielding bPalm-CS (compound **5**, Scheme 1). As characterized by ^{13}C solid-state NMR, bPalm-CS shows the emergence of aliphatic and carbonyl (C═O) signals, as compared to chitosan, at 10−50 and 170−180 ppm, respectively (Figure 2B), confirming the successful conjugation of bPalm groups on the chitosan backbone. The degree of bPalm substitution (DS_{bPalm}) was 2.3% as calculated from the relative ratio between the peak

https://doi.org/10.1021/acsomega.1c06101
ACS Omega 2022, 7, 10056−10068

Scheme 1. Synthesis Procedure of bPalm-CS-HTAP

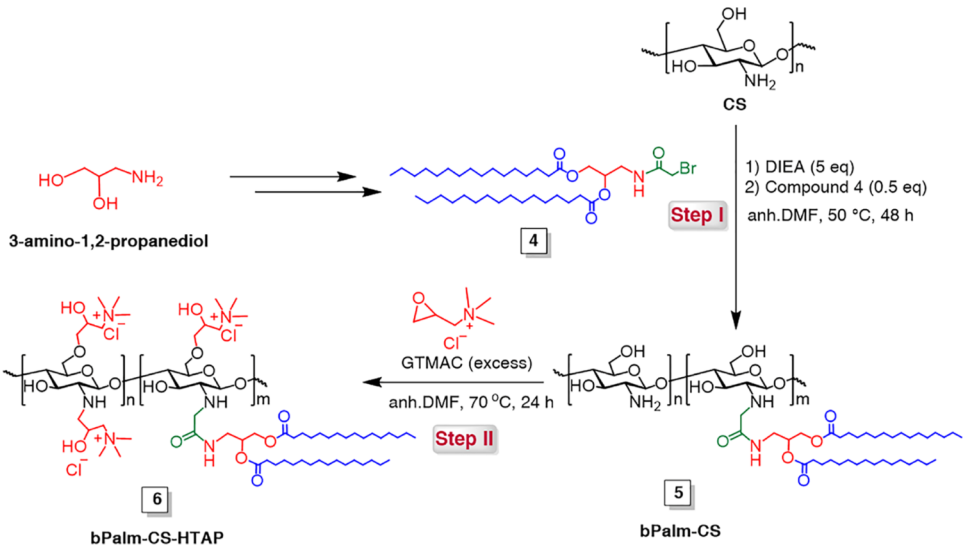

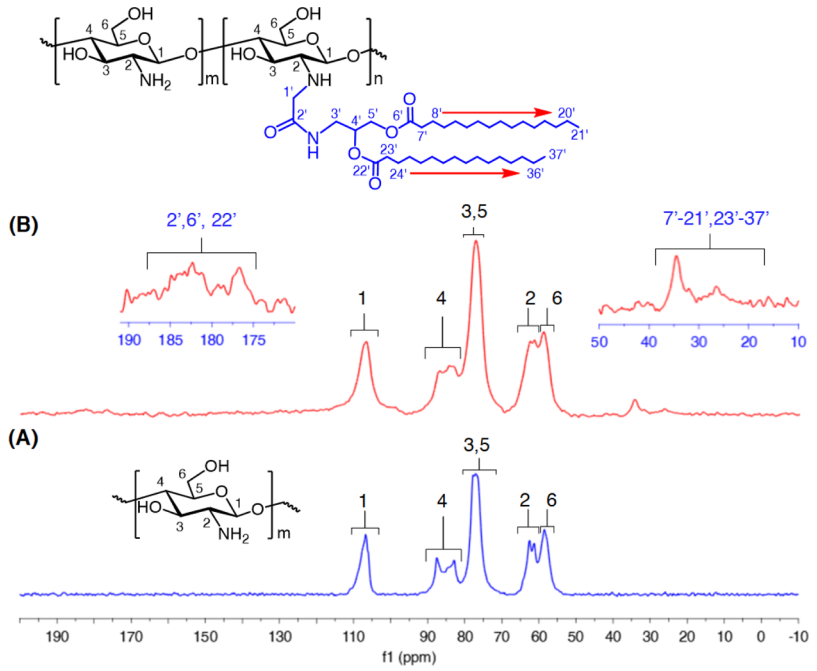

Figure 2. ^{13}C Solid-state NMR spectra (400 MHz) of (A) chitosan and (B) bPalm-CS.

integration of carbonyl carbon belonging to bPalm groups at 170−180 ppm to the peak integration of anomeric carbon of the chitosan backbone at 107 ppm (Figure S15, SI and eq 1). The FT-IR spectrum of bPalm-CS (Figure 3C), in comparison with chitosan (Figure 3A), shows an emergence of new peaks at 1740 and 1595 cm^{-1} and a relative increase in the absorption peak at 2850−2950 cm^{-1}. The signal at 1740 cm^{-1} could be attributed to the carbonyl stretching of bis-palmitoyl ester, while the signals at 1595 and 2850−2950 cm^{-1} could be respectively assigned to the N−H stretching of a secondary amine and the C−H stretching of aliphatic bis-palmitoyl chains in the bPalm units. These functional group assignments align with the FT-IR spectrum observed with the precursor of the bPalm unit (Figure 3B). This evidence confirms the presence of bPalm units in the bPalm-CS.

The reaction of bPalm-CS with GTMAC via nucleophilic ring-opening of epoxide gave bPalm-CS-HTAP. Due to the low DS_{bPalm} at C2-NH_2, GTMAC could react with both hydroxyl (C6-OH) and unreacted amino (C2-NH_2) groups, allowing HTAP units to attach at both C2 and C6 positions of chitosan (Figure 1). As shown in Figure 4, the ^{1}H NMR spectrum of the bPalm-CS-HTAP shows the emergence of signals centered at 0.78, 1.19, and 3.33 ppm. The signals at 0.78 and 1.19 ppm are attributed to methylene ($-CH_2-$) protons and methyl ($-CH_3$) protons of the aliphatic bis-palmitoyl chains. The signal at 3.33 ppm, as reported previously by Silva *et al.*,[59] is assigned to methyl protons of quaternary ammonium ($-N^+(CH_3)_3$) groups, suggesting the successful installation of the HTAP unit on the chitosan backbone. The signals of palmitoyl protons and *N*-acetyl protons in the range of 2.43−4.56 ppm that could overlap with

https://doi.org/10.1021/acsomega.1c06101
ACS Omega 2022, 7, 10056−10068

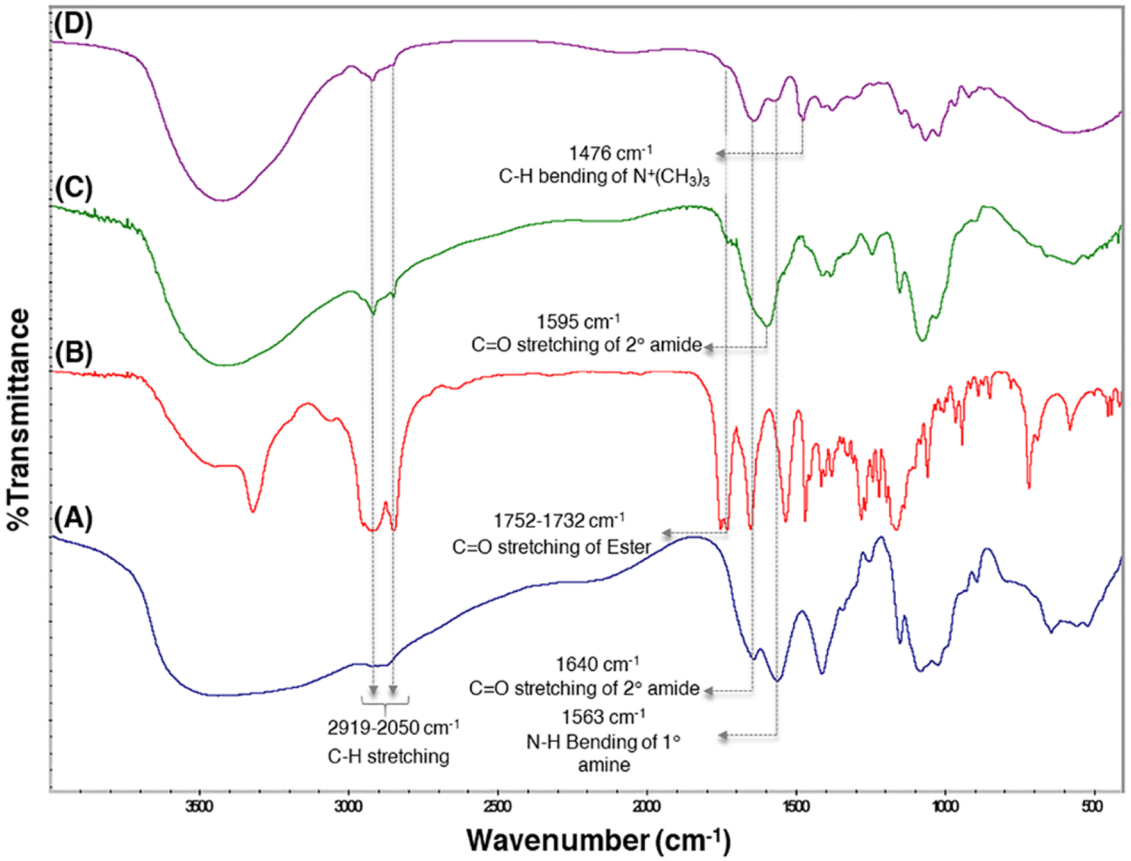

Figure 3. FT-IR spectra (KBr, cm^{-1}) of (A) chitosan, (B) compound **4**, (C) bPalm-CS, and (D) bPalm-CS-HTAP.

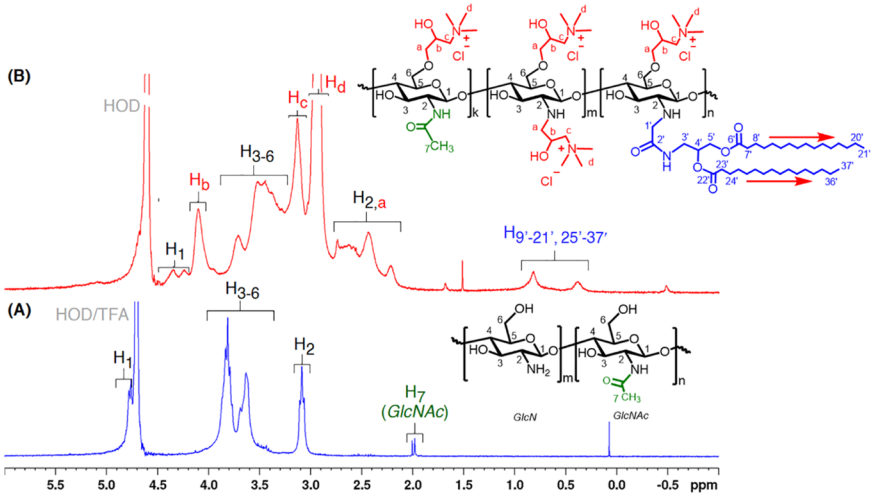

Figure 4. ^{1}H NMR spectra (400 MHz) at 298 K of (A) chitosan (in D_2O/TFA) and (B) bPalm-CS-HTAP (in D_2O).

glucosamine protons were omitted due to the small percentage of DS_{bPalm} of 2.3% and the small degree of acetylation of chitosan (*DA* of 2.3% from ^{1}H NMR, Figure S16, SI), as to further simplify the calculation. The degree of quaternization (*DQ*) of approximately 56.2% was calculated from the relative ratio between the peak integration of Hb of HTAP units at 4.24 ppm and the peak integration of glucosamine protons (H1−H6) at 2.48−4.47 ppm (Figure S17, SI and eq 3). Due to the signal overlap of Hb with glucosamine protons that could affect the proton integrated values, conductometric titration of bPalm-CS-HTAP with silver nitrate ($AgNO_3$) was also performed to additionally confirm the *DQ*. The result from conductometric titration showed that bPalm-CS-HTAP gave a *DQ* of 41.4% (Figure S18, SI), which is close to the value obtained from ^{1}H NMR analysis. This reassures the number of quaternary ammonium groups of about half of the number of monomer units in the polymer chain. In addition, we also analyzed the DS_{bPalm} from the ^{1}H NMR spectrum of bPalm-CS-HTAP. Aligned with the result obtained from ^{13}C solid-state NMR analysis of bPalm-CS, the DS_{bPalm} of about 1.1% was calculated based on the relative ratio between the peak integration of H9′−H21′ and H25′−H37′ of bPalm units at

https://doi.org/10.1021/acsomega.1c06101
ACS Omega 2022, 7, 10056−10068

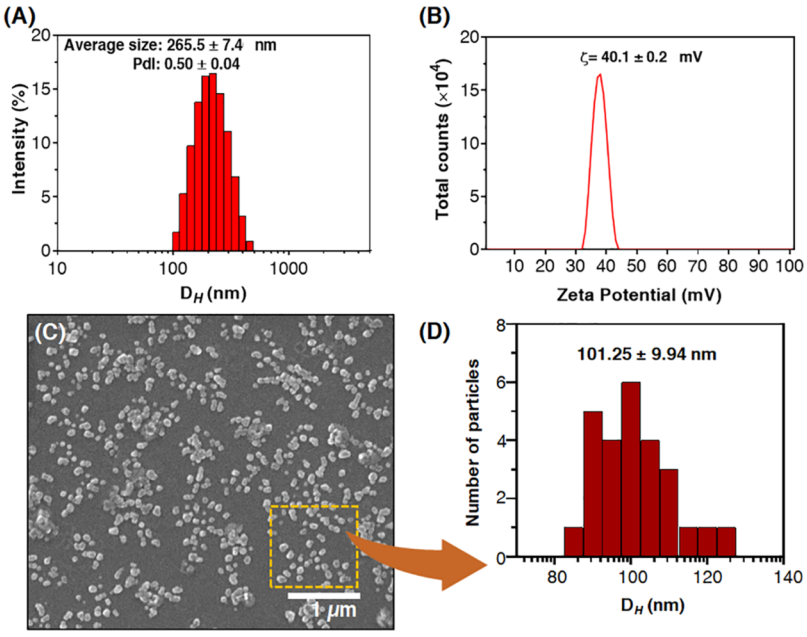

Figure 5. Results of DLS measurement of 7.6 mM bPalm-CS-HTAP in water for (A) particle size distribution, (B) zeta potential distribution, (C) SEM image of 8.3 mM bPalm-CS-HTAP in water deposited on a glass slide and coated with gold, and (D) histogram of particle size distribution as evaluated by SEM.

0.18−1.71 ppm and the peak integration of glucosamine protons (H1−H6) at 2.43−4.56 ppm (Figure S17, SI and eq 2). The FT-IR spectrum of bPalm-CS-HTAP shows a strong signal at 1477 cm^{-1}, which is assigned to the C−H bending of $-N^{+}(CH_3)_3$ (Figure 3D).[60,61] This evidence additionally confirmed the successful installation of HTAP units on the chitosan backbone.

2.2. Characterization of Self-Assembled bPalm-CS-HTAP Particles. As evidenced by DLS, the amphiphilic bPalm-CS-HTAP was found to assemble into nanosized particles in water with a hydrodynamic diameter (D_H) of 265.5 ± 7.4 nm (PDI = 0.50 ± 0.04) and a zeta potential of 40.1 ± 0.2 mV (Figure 5A,B). SEM analysis revealed that bPalm-CS-HTAPs arranged themselves in a spherical shape with an average size of 101.25 ± 9.94 nm (Figure 5C,D). The reduction in size of bPalm-CS-HTAP observed by SEM as compared with DLS could be explained by the fact that SEM analysis was performed under nonhydrated conditions of which particles are dried and well separated, whereas the DLS measurement was conducted under hydrated conditions so that the hydration layer and aggregation of particles have to be taken into account for the average size result.[62,63] The positively charged surface of the particles suggests that bPlam-CS-HTAP arranges HTAP moieties on the outside of the assembled structure, providing binding sites for nucleic acid cargos. The nanosized dimension (100−250 nm) and the positive zeta potential made bPalm-CS-HTAP desirable materials for effective gene carriers.[64−66]

2.3. Electrophoretic Mobility Shift Assay. To determine the optimal complexation condition, it is necessary to evaluate the condensation capability of bPalm-CS-HTAP with pDNA at different bPalm-CS-HTAP/pDNA ratios. In this study, we utilized the mammalian expression plasmid pVAX1.-COV2RBDme to study the condensation capability of bPalm-CS-HTAP. This plasmid carries *COV2RBDme*, a gene encoding a chimeric protein designed from the proteins of SARS-CoV-2 and containing the V5 tag to facilitate protein detection. The complex formation of bPalm-CS-HTAP/pDNA was visualized by electrophoretic mobility shift assay (EMSA) with the constant amount of pDNA at 0.2 μg/well and a varied amount of bPalm-CS-HTAP to give bPalm-CS-HTAP/pDNA weight ratios of 0.1, 0.2, 0.3, 0.4, 0.5, 0.6, 0.7, 0.8, 0.9, 1, 2, 3, and 4 (Figure 6). The result showed the decreased intensity of

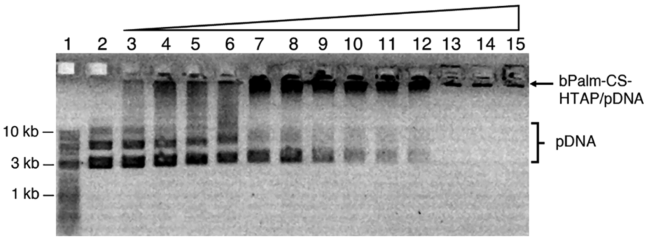

Figure 6. Gel electromobility shift assay (EMSA) of bPalm-CS-HTAP/pDNA polyplexes. pDNA (0.2 μg) was mixed with bPalm-CS-HTAP at different weight ratios prior to DNA separation using 0.8% agarose in 0.5× Tris-acetate-EDTA running buffer. Lanes 1 and 2 are the DNA marker and free pDNA, respectively, and lanes 3−15 are bPalm-CS-HTAP/pDNA polyplexes at weight ratios of 0.1, 0.2, 0.3, 0.4, 0.5, 0.6, 0.7, 0.8, 0.9, 1, 2, 3, and 4, respectively.

the free pDNA band with the increasing weight ratio of bPalm-CS-HTAP:pDNA. The DNA band disappeared completely at the bPalm-CS-HTAP/pDNA weight ratio of 2:1 (Figure 6, lane 13), indicating the complete binding of pDNA to bPalm-CS-HTAP. The complexation between pDNA and bPalm-CS-HTAP is a result of electrostatic interaction between the positively charged bPalm-CS-HTAP and the negatively charged pDNA.

2.4. Cytotoxicity of bPalm-CS-HTAP. Cellular toxicity is critical for polymeric vectors for *in vivo* and clinical applications. The cytotoxicity of bPalm-CS-HTAP was examined using two different methods: trypan blue staining and CCK-8 assay. HEK 293A cells grown in 12-well plates were transfected with bPalm-CS-HTAP complexed with 1 μg

https://doi.org/10.1021/acsomega.1c06101
ACS Omega 2022, 7, 10056−10068

of pDNA into weight ratios of 0.1, 0.3, 0.5, 1, 3, 5, 10, 20, 30, and 40 that resulted in the total concentration of 2 ng/μL pDNA and 0.2−80 ng/μL bPalm-CS-HTAP (Figure 7A). Live

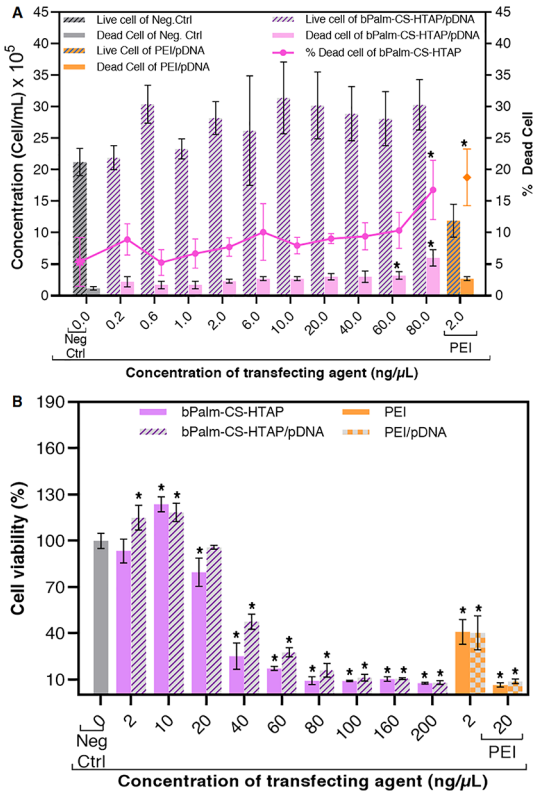

Figure 7. Cytotoxicity test of bPalm-CS-HTAP. (A) Trypan blue staining of HEK 293A cells transfected with 1 μg of pDNA mixed with 0.2−80 ng/μL bPalm-CS-HTAP in 12-well plates. (B) CCK-8 assay of HEK 293A transfected with 0.1 μg of pDNA mixed with 2−200 ng/μL bPalm-CS-HTAP. Transfections with 2−10 ng/μL PEI were included. Data represent the mean ± SD (n = 3). The asterisk (*) indicates a significant difference (P < 0.05), in comparison with "Neg Ctrl".

and dead cells were then determined by staining with trypan blue at 48 h post-transfection and were used for the calculation of percentage of dead cells. While the negative control (pDNA without a transfection reagent) exhibited 5.3 ± 1.8% cell death, a low amount of bPalm-CS-HTAP with the concentration from 0.2 to 60 ng/μL resulted in cell death lower than 11% (5.3 ± 2.0 to 10.4 ± 2.9%). An increased concentration of bPalm-CS-HTAP to 80 ng/μL caused more dead cells up to 16.8 ± 4.7%; however, cells transfected with 2 ng/μL PEI were found to give the highest cell death of 18.8 ± 4.5%. This suggested that the transfection of HEK 293A cells with bPalm-CS-HTAP at concentrations of 0.1−80 ng/μL and PEI at a concentration of 2 ng/μL in 12-well plates ensures a decent amount of cell viability of up to 75%.

To evaluate the toxicity of bPalm-CS-HTAP in the presence and absence of pDNA, we performed CCK-8 assay of bPalm-CS-HTAP against HEK 293A cells in a broader range of concentrations. The assay was performed using the cells grown in 96-well plates and with various concentrations of bPalm-CS-HTAP of 2, 10, 20, 40, 60, 80, 100, 160, and 200 ng/μL, either in the presence or absence of 2 ng/μL pDNA (Figure 7B). The cell viability was determined using the CCK-8 reagent at 48 h post-transfection. The result showed that bPalm-CS-HTAP enhanced the cell viability (123.6 ± 4.8 to 132.7 ± 2.2% cell viability) at low concentrations (2−10 ng/μL) and decreased the cell viability (74.6 ± 4.6 to 3.0 ± 1.0% cell viability) at the higher concentrations (>10 ng/μL) in a concentration-dependent manner. PEI (20 kDa, 20 ng/μL) exhibited a higher toxicity than bPalm-CS-HTAP at the same concentration. Interestingly, the toxicity of bPalm-CS-HTAPs decreased when they form a complex with pDNA up to 88.8%, suggesting that pDNA can neutralize the toxicity of bPalm-CS-HTAP. Interacting with negative charges of pDNA, the excess cationic surface charge of bPalm-CS-HTAP particles can be nullified. Hence, the polyplexes are not expected to efficiently bind electrostatically to the cell matrix and the cell surface.[67,68] Compared to the trypan blue staining method, the CCK-8 assay showed a higher toxicity of bPalm-CS-HTAP/pDNA complexes as the concentration increased as well. However, the CCK-8 assay resulted in a higher toxicity of bPalm-CS-HTAP at 40−80 ng/μL (25.2 ± 8.5 to 10.4 ± 1.5% cell viability), in comparison with the trypan blue method (9.4 ± 2.2 to 16.8 ± 4.7% dead cells). Since the cytotoxicity measurements of the trypan blue method and the CCK-8 assay are based on cell membrane permeability and enzyme activity, respectively,[69,70] the trypan blue method is not sensitive to injured cells that lost cell functions but still maintained their membrane integrity.[71] Therefore, the higher toxicity of bPalm-CS-HTAP observed with the CCK-8 assay, in comparison with the trypan blue method, suggested that bPalm-CS-HTAP could impair cell functions while keeping the cells alive at high concentrations (>40 ng/μL).

Evidence of cell growth enhancement in the presence of bPalmCS-HTAP at low carrier concentrations could be explained by the inherent mucoadhesive property of chitosan, leading to cell attachment and proliferation to a greater extent.[72,73] However, when the concentration of bPalm-CS-HTAP increased, the permanent positive charge of the quaternary ammonium groups could result in excess electrostatic interactions with the plasma membrane of the cells, which cause aggregation of bPalm-CS-HTAP on the cell surfaces, thus impairing the cell membrane function and leading to cell death.[29,31,60,74,75]

2.5. *In Vitro* Gene Transfection. The ability of bPalm-CS-HTAP to assist the transfection of pDNA into mammalian cells was evaluated. Transfection was performed in HEK 293A and CHO cells with the plasmid pVAX1.CoV2RBDme. The transfection efficiency was determined by the level of the V5-tagged CoV2RBDme expressed by pDNA upon cell transfection using the immunofluorescence technique. The amphiphilicity of bPalm-CS-HTAP allows both electrostatic and hydrophobic interactions to give pDNA condensation and self-assembled nanoparticles, improving the cellular uptake and stability of pDNA against nuclease degradation.[37,38,74] After incubation with bPalm-CS-HTAP/pDNA complexes at weight ratios of 3:1, 5:1, 10:1, 20:1, and 40:1 and a pDNA concentration of 2 ng/μL for 48 h, cells were stained with a rabbit anti-V5 primary antibody followed by goat antirabbit IgG conjugated with an Alexa Fluor 488 secondary antibody to determine the expression of the CoV2RBDme protein. Cells treated with naked pDNA (negative control) showed no fluorescence, while cells treated with PEI/DNA (positive control) yielded the highest intensity of green fluorescence among all transfection conditions (Figure 8). These results indicate that there was no pDNA uptake or successful pDNA translation without carriers, while PEI efficiently mediated

https://doi.org/10.1021/acsomega.1c06101
ACS Omega 2022, 7, 10056−10068

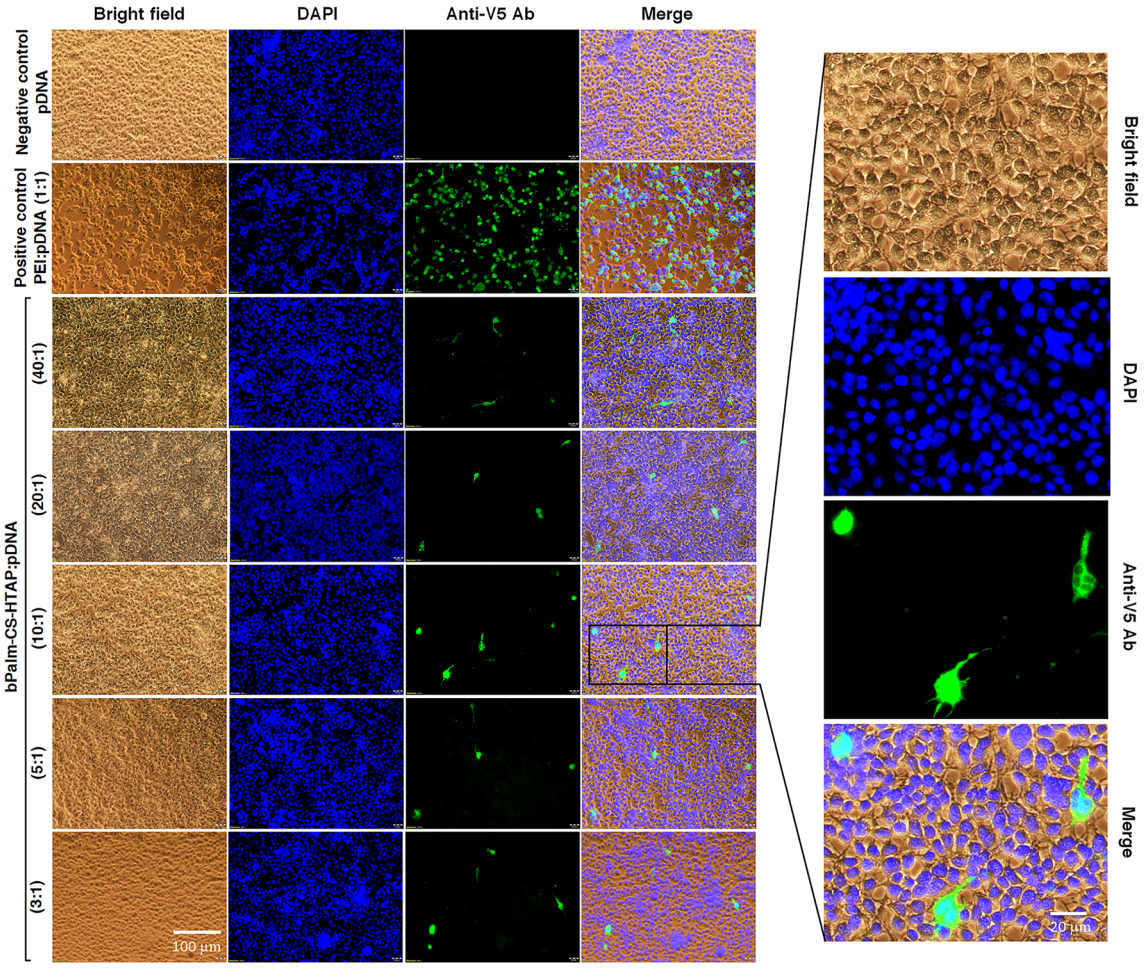

Figure 8. Fluorescence images of HEK 293A cells treated with bPalm-CS-HTAP complexed with the plasmid DNA. Transfection was performed with bPalm-CS-HTAP/pDNA at weight ratios of 3:1, 5:1, 10:1, 20:1, and 40:1. Transfection conditions with PEI/pDNA (1:1) and naked pDNA were included as a positive and negative control, respectively. Cells were indicated by the bright-field (BF) image. The nuclei of the cells were stained with DAPI, and the expressed CoV2RBDme protein was detected using a rabbit anti-V5 antibody followed by goat antirabbit IgG conjugated with Alexa Fluor 488. Fluorescence images were observed using a fluorescence microscope.

pDNA uptake as seen by a high level of protein expression. Cells treated with bPalm-CS-HTAP/pDNA complexes showed fluorescence of the CoV2RBDme protein at the minimum bPalm-CS-HTAP/pDNA ratio of 3:1; however, we did not observe an increased green fluorescence signal when the ratio of bPalm-CS-HTAP:pDNA was elevated up to 40:1 (Figure 8). Compared to the fluorescence intensity in the cells treated with the PEI/pDNA polyplex, the fluorescence intensity in the cells treated with bPalm-CS-HTAP/pDNA polyplexes was considerably lower, even at the elevated bPalm-CS-HTAP concentration that the greater amount of pDNA delivered into cells was expected. We also performed the transfection of bPalm-CS-HTAP/pDNA with the CHO cell line, and the minimum bPalm-CS-HTAP/pDNA ratio of 3:1 that generated the expression of the CoV2RBDme protein was also observed. Based on the green fluorescence signal, the transfection efficiency in CHO cells was slightly lower than that in HEK 293A cells at all conditions and was not improved with the increased ratio of bPalm-CS-HTAP/pDNA (Figure S19, SI). We hypothesized that the low transfection efficiency of bPalm-CS-HTAP could be due to the tight binding between bPalm-CS-HTAP and pDNA via electrostatic interactions as mentioned above. This strong interaction between bPalm-CS-HTAP and pDNA resulted in an insufficient release of pDNA from the bPalm-CS-HTAP/pDNA complexes, thus impeding the expression of pDNA. In addition, the toxicity of bPalm-CS-HTAP as the concentration increased (Figure 7B) could disrupt various cellular functions including protein synthesis, leading to poor gene expression at a higher bPalm-CS-HTAP:pDNA ratio.[74] Xiao et al. reported that a quaternized chitosan with a *DQ* of 43.7%, a similar *DQ* to that of bPalm-CS-HTAP (*DQ* of 56%), gave an about 10^5-fold lower transfection efficiency of the transfecting plasmid pGL3 into Hela cells, compared to EndoFectin-Lenti, a commercial transfecting agent. Upon the reduction of the *DQ* to 12.4%, the transfection efficiency was improved by about 1000-fold.[74] These pieces of evidence suggest that bPalm-CS-HTAP could suffer from having too much positive charge that leads to modest gene expression. The presence of hydrophobic bPalm groups with a DS_{bPalm} of 2% seems to be not enough to rescue the transfection performance of the quaternized chitosan carrier. It was also reported that the hydrophobic part of amphiphiles could weaken the electrostatic interaction between cationic carriers and their nucleic acid cargos.[76] To further improve the transfection efficiency of bPalm-CS-HTAP, the *DQ* and the DS_{bPalm} should be modulated to an optimum point with a lower *DQ* and a higher DS_{bPalm} that the amphiphile can still retain its aggregation into nanosized

https://doi.org/10.1021/acsomega.1c06101
ACS Omega 2022, 7, 10056−10068

particles with a decreased surface charge density while maintaining its aqueous solubility. The observed green fluorescence in the cell samples treated with bPalm-CS-HTAP/pDNA complexes indicates that bPalm-CS-HTAP has the potential to be further developed as a pDNA carrier.

3. CONCLUSIONS

The amphiphilic chitosan bPalm-CS-HTAP was successfully synthesized by attaching the *N*-(2-((2,3-bis(palmitoyloxy)-propyl)amino)-2-oxoethyl) (bPalm) group and the *O*-[(2-hydroxyl-3-trimethylammonium)] propyl (HTAP) group to the chitosan backbone. The resulting bPalm-CS-HTAP with a DS_{bPalm} of 2% and a *DQ* of 56% gave well-defined and nanosized spherical particles with a hydrodynamic diameter (D_H) of 265.5 ± 7.40 nm (PDI = 0.50) and a surface charge potential of +40.1 ± 0.20 mV. The positively charged surface of bPalm-CS-HTAP enabled complexation with the plasmid DNA as observed in EMSA. While bPalm-CS-HTAP/pDNA complexes gave a cell viability of up to 80% at 0.1−80 ng/μL by the trypan blue staining method, it showed a higher toxicity in the CCK-8 assay at above 40 ng/μL due to its effect of disrupting cell functions. The *in vitro* transfection of bPalm-CS-HTAP/pDNA into HEK 293A and CHO cells showed similar modest protein expression levels with negligible cytotoxicity, compared to PEI at the same concentration. We hypothesize that the low transfection efficiency of bPalm-CS-HTAP is due to the high positive surface charge of bPalm-CS-HTAP particles that impeded the release of pDNA from the polyplexes. Although bPalm-CS-HTAP yields a lower transfection efficiency, in comparison with PEI, it has a merit of a much lower cytotoxicity and the chance to improve its transfection performance by balancing the hydrophobicity and hydrophilicity. The result obtained from this work demonstrates that bPalm-CS-HTAP has the potential to be used as a vector for gene delivery. A further investigation into the effect of DS_{bPalm} and *DQ* could be performed to improve the transfection efficacy and reduce the toxicity of the material.

4. MATERIALS AND METHODS

4.1. Materials. Chitosan (CS, M_w of 100 kDa, degree of deacetylation of 95%) was purchased from Seafresh Chitosan Lab Co., Ltd. (Thailand). All reagents were received from Sigma-Aldrich (USA) and Tokyo Chemical Industry (TCI, Japan). Analytical-grade solvents were purchased from Sigma-Aldrich, Merck, Honeywell, QReC, Fisher Chemical, and RCI Labscan (Thailand). Commercial-grade solvents were purchased from Biotech and Scientific Co., Ltd. (Thailand) and RCI Labscan (Thailand). Distillation was performed to dry dichloromethane before use. The moisture-sensitive reactions were performed under a nitrogen atmosphere (Praxair, Thailand). Thin-layer chromatography (TLC) was used to monitor the reaction's progress and visualize it under UV light (365 nm). Commercial-grade solvents such as dichloromethane, ethyl acetate, and hexane were used for extraction and column chromatography without additional purification. All aqueous solutions of samples were prepared using type I water (Ultrapure). Phosphate-buffered saline (PBS, Sigma) was diluted in distilled water to 1× dilution before usage. ADT was the mixture of adenosine (0.5% w/v), deoxyadenosine (0.5% w/v), and thymidine (0.5% w/v), which were purchased from Sigma, USA. Dulbecco's modified Eagle's medium (DMEM) was purchased from HIMEDIA, India. Fetal bovine serum (FBS) was purchased from Hyclone, New Zealand. D-Glucose was purchased from Gibco, USA. L-Glutamine was purchased from HIMEDIA, India. The HEK 293A cell line was purchased from Invitrogen, USA. CHO cells were purchased from ATCC, USA. pVAX1.CoV2RBDme DNA, encoding the V5-tagged protein, was generated in the Animal Cell Culture lab (KMUTT, Thailand). A Cell Counting Kit-8 (CCK-8) was purchased from Dojindo, Japan.

4.2. Synthesis of Chitosan Having *N*-(2-((2,3-Bis-(palmitoyloxy)propyl)amino)-2-oxoethyl) (bPalm) Groups (bPalm-CS). Chitosan (3.0 g) was dissolved in anhydrous *N*,*N*-dimethylformamide (60 mL) in a round-bottom flask at 50 °C under a nitrogen atmosphere for three days (500 mg of chitosan was dissolved to give 3.106 mmol of $-NH_2$). Following Step I, Scheme 1, compound **4** (2.139 g, 3.106 mmol) of which the synthesis and characterization are provided in the SI and *N*,*N*-diisopropylethylamine (1.08 mL, 6.211 mmol) were then dissolved in DMF and subsequently added dropwise (60 min) into the chitosan solution. The reaction was continued at 50 °C for 48 h, and the reaction mixture was filtered to remove undissolved chitosan. The filtrate was dialyzed (M_W cutoff of 12,000 Da) against distilled water for three days and lyophilized to obtain a yellowish crude product and washed several times with dichloromethane to remove unreacted compound **4** and dried *in vacuo*. A light yellow powder of bPalm-CS was obtained as the product (59.58% yield). ^{13}C NMR (solid-state) δ (ppm) = 176 (carbonyl carbon of ester: C2′, C6′, and C22′), 106 (anomeric carbon: C1), 87−59 (glucosamine carbon: C2−C6 and palmitoyl unit: C1′, C3′−C5′), 34−36 (carbon of the palmitoyl chain: C7′−C21′, C23′−C37′). FT-IR (KBr pellet) υ = 3442 cm^{-1} (O−H stretching of glucosamine), 2850−2950 cm^{-1} (C−H stretching of hydrocarbon), 1740 cm^{-1} (C═O stretching of ester), 1640 cm^{-1} (C═O stretching of 2° amide), 1595 cm^{-1} (N−H bending of amine), 1412 cm^{-1} (O−H bending of alcohol), and 1076 cm^{-1} (C−O stretching of the secondary alcohol).

4.3. Synthesis of Chitosan Having *N*-(2-((2,3-Bis-(palmitoyloxy)propyl)amino)-2-oxoethyl) and *O*-[(2-Hydroxyl-3-trimethylammonium)] Propyl Groups (bPalm-CS-HTAP). bPalm-CS (50 mg, 0.065 mmol) was reacted with glycidyltrimethylammonium chloride (GTMAC) (1.972 g, 13 mmol) in anhydrous *N*,*N*-dimethylformamide (3 mL) in a round-bottom flask (10 mL); then, the reaction mixture was heated to 70 °C under a nitrogen atmosphere for 24 h (Step II, Scheme 1). Subsequently, the reaction mixture was dialyzed against distilled water for three days and lyophilized to yield the yellowish powder of bPalm-CS-HTAP (91.37% yield). ^1H NMR (400 MHz, D_2O, 298 K) for bPalm-CS-HTAP: δ (ppm) = 4.47−4.36 (H1), 4.26 (Hb), 3.87−3.33 (H3−H6, Hc), 3.16 ($-N^+(CH_3)_3$), 2.97−2.48 (H2, Ha), 1.19−0.02 (H9′−H21′, H25′−H37′). FT-IR (KBr pellet) υ = 3423 cm^{-1} (O−H stretching of HTAP groups, glucosamine), 2920−2852 cm^{-1} (C−H stretching of hydrocarbon), 1740 cm^{-1} (C═O stretching of ester), 1640 cm^{-1} (C═O stretching of 2° amide), 1563 cm^{-1} (N−H bending of amine), 1476 cm^{-1} (C−H bending of $-N^+(CH_3)_3$, and 1066 cm^{-1} (C−O stretching of ether).

4.4. Chemical Structure Characterization. High-resolution electrospray ionization mass spectra (HRMS) were analyzed on a Bruker MicrOTOF-QII mass spectrometer, measuring both the positive and negative ionization modes. The HRMS data were analyzed by Bruker Daltonics Data

https://doi.org/10.1021/acsomega.1c06101
ACS Omega 2022, 7, 10056−10068

Analysis 3.3. A nuclear magnetic resonance (solid-state NMR: 400 MHz) model JNM-ECZ-400R/S1 was used for ^{13}C solid-state NMR experiments. The chemical shift of ^{13}C spectra was calibrated with the external standard hexamethyl benzene (HMB). The degree of bis(palmitoyloxy)propyl)amino)-2-oxoethyl substitution (DS_{bPalm}) of bPalm-CS was calculated according to eq 1.[77]

$$DS_{bPalm}\ (\%) = \frac{I_{(C=O)}/3}{I_{(C1)}/1} \times 100 \quad (1)$$

where $I_{(C=O)}$ is the signal integral of the carbonyl carbon present in bPalm units at 176−190 ppm, while $I_{(C1)}$ is the anomeric carbon of the glucosamine ring at 107 ppm.

The ^1H and ^{13}C NMR analyses were performed by a Bruker AVANCE II HD spectrometer (400 MHz for ^1H nuclei and 100 MHz for ^{13}C nuclei) at 25 °C. The samples were dissolved in deuterated water (D_2O), a mixture of trifluoroacetic acid/deuterated water (CF_3COOH/D_2O), and deuterated chloroform ($CDCl_3$) for the analyses. The spectra were analyzed using the Topspin 3.6.1 software by Bruker BioSpin. The degree of substitution of bPalm units in bPalm-CS-HTAP was calculated using eq 2.[59,60,77,78]

$$DS_{bPalm}\ (\%) = \frac{I_{H(palmitoyl)}/54}{(I_{HTAP\&CS})/(7 + (DQ \times 14))} \times 100 \quad (2)$$

where $I_{H(palmitoyl)}$ is the signal integral of H9′−H21′ and H25′−H37′ assigned to the bis-palmitoyl substituent in a range of 0.18−1.71 ppm, while $I_{HTAP\ \&\ CS}$ is the signal integral of protons of the HTAP unit and the glucosamine ring from a signal in a range of 2.43−4.56 ppm. The degree of quaternization (DQ) of bPalm-CS-HTAP was calculated according to eq 3.[11]

$$DQ\ (\%) = \frac{I_{H_b}/1}{[I_{H_{HTAP\&CS}} - (I_{H_{HTAP}})]/7} \times 100 \quad (3)$$

I_{H_b} is the signal integral of the H_b of HTAP units centered at 4.24 ppm; $I_{H_{HTAP\ \&\ CS}}$ is the signal integral of protons of the HTAP unit and the glucosamine ring from signals in a range of 2.43−4.56 ppm. $I_{H_{HTAP}}$ is the signal integral of H_{a-d}, which equals $I_{H_b} \times 14$.

Infrared spectra were recorded using a Thermo Fisher Scientific spectrometer (model Nicolet 8700, USA), scanning from 4000 to 400 cm^{-1} (% transmittance mode, 32 scans, 4.0 resolution, and 0.4 cm^{-1} data spacing) at room temperature. Samples were mixed separately with KBr powder and manually pressed into pellets for analysis. The background (air) was taken before each sample analysis. The spectra were analyzed in the OMNIC 8.3.103 software by Thermo Fisher Scientific, Inc.

4.5. Nanoparticle Characterization. The particle size and the zeta potential of self-assembled bPalm-CS-HTAP were measured using a dynamic light scattering technique (Nano-Partica SZ 100 series, Horiba Scientific, Japan) equipped with a doubled laser (532 nm, 10 mW) and a PMT detector operating at 25 °C. The measurements were performed at a concentration range of 1−5 wt % (Milli Q water, 1 mL) with a particle size ranging from 0.3 nm to 8 μm (90°) for the size measurement and −200 to +200 mV for the zeta potential measurement.

The morphology of the self-assembled bPalm-CS-HTAP was determined by a scanning electron microscope (SEM, JEOL JSM-6610 LV, Japan). The sample was diluted in water and dropped on a glass plate and dried overnight. The sample was then coated with gold by a sputter-coater (Crossington Model 108 Auto, JEOL, Japan) and subsequently observed and photographed.

4.6. Gel Electrophoresis. bPalm-CS-HTAP/pDNA polyplexes were prepared at varied bPalm-CS-HTAP:pDNA ratios by mixing 0.02−0.8 μg of bPalm-CS-HTAP with 0.2 μg of pDNA in a 10 μL total volume of 1× PBS. The mixtures were mixed well by vortexing and incubated at room temperature for 15 min to enable complexation. Then, Purple (6×), no SDS (New England Biolabs) (2 μL), was added to each tube, and 12 μL of the mixture was loaded into a 0.8% agarose gel. The samples were subsequently analyzed in an electric field of 135 V using 0.5× TAE buffer (40 mM Tris/acetate and 1 mM EDTA) as a running buffer for 14 min. After electrophoresis, the gel was stained with ethidium bromide and washed with distilled water. The gel was observed under UV light (200 AZURE Biosystems, USA).

4.7. Cytotoxicity Assay. The cytotoxicity of bPalm-CS-HTAP was evaluated by two methods using trypan blue staining and Cell Counting Kit-8 (CCK-8) by the following procedures.

For trypan blue staining, HEK 293A cells were transfected with bPalm-CS-HTAP/pDNA complexes in 12-well plates following the same procedure as in the transfection part. After the cells were treated with the polyplexes and incubated for a total of 48 h, the medium was collected, and the cells were treated with 450 μL of 0.25% trypsin-1× EDTA for 2−3 min followed by pipetting the detached cells into a 1.5 mL microcentrifuge tube. Trypsinized cells and cells collected from the old media were centrifuged at 1200 rpm for 3 min at room temperature. The supernatants were decanted, and the cell pellets were suspended in 500 μL of complete DMEM and mixed well. The suspended cells (5 μL) were treated with 20 μL of a trypan blue dye, and the cells were counted for live and dead cells in triplicate for each transfection condition under a hemocytometer. Cell concentrations (C) were calculated according to eq 4.

$$C_{cell}\ (cell/mL) = cell \times dilution\ factor \times 10^4 \quad (4)$$

The percentage of dead cells was calculated according to eq 5.

$$\%\ dead\ cell = \frac{C_{dead\ cells}}{(C_{live\ cells} + C_{dead\ cells})} \times 100 \quad (5)$$

where C is concentration.

For the CCK-8 assay, the cytotoxicities of bPalm-CS-HTAP and bPalm-CS-HTAP/pDNA were evaluated with HEK 293A cells. Cells were seeded into 96-well culture plates at a density of 5×10^3 cells per well and maintained in complete DMEM. After incubation at 37 °C in a humidified atmosphere containing 5% CO_2 for 24 h, the old medium was removed, and the cells were treated with 50 μL of bPalm-CS-HTAP and bPalm-CS-HTAP/pDNA resuspended in serum-free DMEM at bPalm-CS-HTAP concentrations of 2, 10, 20, 40, 60, 80, 100, 160, and 200 ng/μL and a pDNA concentration of 2 ng/μL. Cells treated with PEI/pDNA at 2 and 20 ng/μL PEI and 2 ng/μL pDNA served as a positive control, while nontreated cells in 50 μL of serum-free DMEM served as a negative control (100% cell viability). After incubation for 4 h in the

https://doi.org/10.1021/acsomega.1c06101
ACS Omega 2022, 7, 10056−10068

serum-free medium, 50 μL of complete DMEM was added to each well, and the incubation was continued for another 44 h. Consequently, the cells were removed from the incubator, and 10 μL of CCK-8 solution was added into each well. After a 2 h incubation with CCK-8 at 37 °C and 5% CO_2, the absorbance was recorded by a microplate reader (Multiskan FC, Thermo Fisher Scientific, USA) at a wavelength of 450 nm (quartz-halogen). The cell viability (%) was calculated according to eq 6.

$$\text{cell viability (\%)} = \frac{\text{absorbance of the sample}}{\text{absorbance of the negative control}} \times 100 \quad (6)$$

4.8. Transfection Assay. Human embryonic kidney (HEK 293A) cells were seeded in 12-well plates at a seeding density of 1 × 10^5 cells/well and incubated in 1 mL of a growth medium containing 90% DMEM, 10% FBS, and 1% pen/strep at 37 °C with 5% CO_2 and grown for 24 h to reach 80−90% confluency prior to transfection. bPalm-CS-HTAP/pDNA polyplexes were prepared at weight ratios of 0.1:1, 0.3:1, 0.5:1, 1:1, 3:1, 5:1, 10:1, 20:1, and 40:1 with the fixed amount of pDNA of 1 μg in a total volume of 10 μL, which was added with 90 μL of serum-free media to reach a final volume of 100 μL each. The polyplexes were incubated at room temperature for 15 min, and another 400 μL of serum-free DMEM was subsequently added. The mixed solution was then transferred into cells that were previously washed with 1× PBS. After incubation for 4 h at 37 °C with 5% CO_2, another 500 μL of complete DMEM was added to each well, and cells were incubated for another 44 h at 37 °C with 5% CO_2.

Chinese hamster ovary (CHO) cells were cultivated in 350 μL of a Minimum Essential Medium Alpha (MEM-Alpha) containing 1% D-glucose, 10% FBS, and 1% L-glutamine and 0.2% ADT mix at 37 °C with 5% CO_2 and incubated for 24 h to reach 80−90% confluency prior to transfection. bPalm-CS-HTAP/pDNA polyplexes were prepared at the same concentration and weight ratio as previously described for the other cell line cultivated in 12-well plates. After 15 min of incubation, the polyplexes were transferred into cells to give the final transfection volume of 300 μL. Subsequently, cells were incubated at 37 °C with 5% CO_2 for 4 h at room temperature followed by an addition of 300 μL of complete MEM-Alpha. The cells were incubated at 37 °C with 5% CO_2 for another 44 h.

Cells added with PEI (linear PEI HCl salt, 20 kDa, Sigma)/pDNA complexes at a weight ratio of 1:1 and a final concentration of 2 ng/μL serve as a positive control, while cells incubated with 2 ng/μL pDNA serve as a negative control. After a total of 48 h of incubation, the transfected cells were fixed with 1% formaldehyde (diluted in PBS) for 10 min at room temperature and washed with PBS. To permeabilize the cell membrane, 90% cold methanol was added to the cells followed by incubation for 5 min at 4 °C. After being washed with PBS, the cells were blocked with 2% FBS diluted in PBS (2% FBS/PBS) for 1 h at room temperature, washed with PBS, and incubated for 1 h at room temperature with a rabbit anti-V5 primary antibody (Abcam) diluted to 1:2000 in 2% FBS/PBS. The cells were subsequently washed twice with PBS and incubated for 2 h at room temperature with a goat antirabbit IgG secondary antibody conjugated with Alexa Fluor 488 (Sigma) diluted to 1:1000 in 2% FBS/PBS. After being washed with PBS, the cell nucleus was stained with 4′,6-diamidino-2-phenylindole (DAPI, Sigma) diluted to 1:2000 in PBS. Following incubation at room temperature for 10 min, the cells were then washed with PBS and examined under an inverted fluorescence microscope (Olympus IX71, Japan) with a 20× objective lens.

4.9. Statistical Analysis. Data are shown as means (±SD) of three replicated experiments, and statistical analysis was performed using one-way ANOVA carried out by the SPSS 17.0 software (SPSS, Inc., Chicago, IL, USA). The degree of the significant difference was set at the probability of $p < 0.05$, which was determined by Tukey's post hoc tests.

■ ASSOCIATED CONTENT

Supporting Information

The Supporting Information is available free of charge at https://pubs.acs.org/doi/10.1021/acsomega.1c06101.

General procedure of the synthesis and characterization of compound **4**, ^{1}H NMR characterization of bPalm-CS and bPalm-CS-HTAP, conductometric titration of bPalm-CS-HTAP, and transfection of bPalm-CS-HTAP/pDNA into CHO cells (PDF)

■ AUTHOR INFORMATION

Corresponding Author

Kornkanya Pratumyot − *Organic Synthesis, Electrochemistry & Natural Product Research Unit, Department of Chemistry, Faculty of Science, King Mongkut's University of Technology Thonburi, Bangkok 10140, Thailand;* orcid.org/0000-0001-7523-6606; Email: kornkanya.pra@kmutt.ac.th

Authors

Thev Pol − *Organic Synthesis, Electrochemistry & Natural Product Research Unit, Department of Chemistry, Faculty of Science, King Mongkut's University of Technology Thonburi, Bangkok 10140, Thailand*

Wunpen Chonkaew − *Sustainable Polymer & Innovative Composite Materials Research Group, Department of Chemistry, Faculty of Science, King Mongkut's University of Technology Thonburi, Bangkok 10140, Thailand*

Lalintip Hocharoen − *Bioprocess Research and Innovation Centre (BRIC), National Biopharmaceutical Facility (NBF), King Mongkut's University of Technology Thonburi (KMUTT), Bangkok 10150, Thailand*

Nakorn Niamnont − *Organic Synthesis, Electrochemistry & Natural Product Research Unit, Department of Chemistry, Faculty of Science, King Mongkut's University of Technology Thonburi, Bangkok 10140, Thailand*

Namphueng Butkhot − *Division of Biotechnology, School of Bioresources and Technology, King Mongkut's University of Technology Thonburi, Bangkok 10150, Thailand*

Yaowaluck Maprang Roshorm − *Division of Biotechnology, School of Bioresources and Technology, King Mongkut's University of Technology Thonburi, Bangkok 10150, Thailand*

Suda Kiatkamjornwong − *FRST, Academy of Science, Office of the Royal Society, Bangkok 10300, Thailand; Office of Research Affairs, Chulalongkorn University, Bangkok 10330, Thailand*

Voravee P. Hoven − *Department of Chemistry, Faculty of Science and Center of Excellence in Materials and Bio-interfaces, Chulalongkorn University, Bangkok 10330, Thailand;* orcid.org/0000-0002-1330-6784

https://doi.org/10.1021/acsomega.1c06101
ACS Omega 2022, 7, 10056−10068

Complete contact information is available at:
https://pubs.acs.org/10.1021/acsomega.1c06101

Author Contributions

T.P. conducted all the experiments and wrote the manuscript. W.C., L.H., and N.N. were consultants of the project. N.B. and Y.M.R. gave guidance and support on cell culture experiments. S.K. and V.P.H. were consultants and provided additional funding. Y.M.R. and V.P.H. wrote and revised some part of the manuscript. K.P. developed the research plan, supervised the whole project, funded the research work, and wrote the manuscript. All authors reviewed the manuscript and gave comments and approved the final version of the manuscript.

Notes

The authors declare no competing financial interest.

■ ACKNOWLEDGMENTS

The authors are grateful to the Government Budget Grant: Fiscal Year 2019 under project number 21876, the Distinguished Professor Grant (DPG6080001 from The Thailand Research Fund), King Mongkut's University of Technology Thonburi (KMUTT Fund), and Petchra Pra Jom Klao Master's Degree Research Scholarship from King Mongkut's University of Technology Thonburi for financial support and the Scientific Instruments Center, School of Science, KMITL for ^{13}C solid-state NMR measurements. We would also like to thank Asst. Prof. Dr. Kittisak Choojun for advice on solid-state NMR analysis.

■ REFERENCES

(1) Ginn, S. L.; Amaya, A. K.; Alexander, I. E.; Edelstein, M.; Abedi, M. R. Gene therapy clinical trials worldwide to 2017: An update. *J. Gene Med.* **2018**, *20*, No. e3015.
(2) Hardee, C. L.; Arévalo-Soliz, L. M.; Hornstein, B. D.; Zechiedrich, L. Advances in Non-Viral DNA Vectors for Gene Therapy. *Genes* **2017**, *8*, 65.
(3) Cao, Y.; Tan, Y. F.; Wong, Y. S.; Liew, M. W. J.; Venkatraman, S. Recent Advances in Chitosan-Based Carriers for Gene Delivery. *Mar. Drugs* **2019**, *17*, 381.
(4) Kritchenkov, A. S.; Andranovitš, S.; Skorik, Y. A. Chitosan and its derivatives: vectors in gene therapy. *Russ. Chem. Rev.* **2017**, *86*, 231−239.
(5) Chen, R.; Zhang, H.; Yan, J.; Bryers, J. D. Scaffold-mediated delivery for non-viral mRNA vaccines. *Gene Ther.* **2018**, *25*, 556−567.
(6) Jiang, X.; Dai, H.; Leong, K. W.; Goh, S. H.; Mao, H. Q.; Yang, Y. Y. Chitosan-g-PEG/DNA complexes deliver gene to the rat liver via intrabiliary and intraportal infusions. *J. Gene Med.* **2006**, *8*, 477−487.
(7) Yu, C.; Kecen, X.; Xiaosai, Q. Grafting Modification of Chitosan. *In Biopolymer Grafting*; Elsevier: 2018, pp. 295−364.
(8) Li, Z.-T.; Guo, J.; Zhang, J.-S.; Zhao, Y.-P.; Lv, L.; Ding, C.; Zhang, X.-Z. Chitosan-graft-polyethylenimine with improved properties as a potential gene vector. *Carbohydr. Polym.* **2010**, *80*, 254−259.
(9) Ni, R.; Feng, R.; Chau, Y. Synthetic Approaches for Nucleic Acid Delivery: Choosing the Right Carriers. *Life* **2019**, *9*, 59.
(10) Safari, S.; Dorkoosh, F. A.; Soleimani, M.; Zarrintan, M. H.; Akbari, H.; Larijani, B.; Tehrani, M. R. N-Diethylmethyl chitosan for gene delivery to pancreatic cancer cells and the relation between charge ratio and biologic properties of polyplexes via interpolations polynomial. *Int. J. Pharm.* **2011**, *420*, 350−357.
(11) Balazs, D. A.; Godbey, W. Liposomes for use in gene delivery. *J. Drug Delivery* **2011**, *2011*, 326497.
(12) Alameh, M.; Lavertu, M.; Tran-Khanh, N.; Chang, C.-Y.; Lesage, F.; Bail, M.; Darras, V.; Chevrier, A.; Buschmann, M. D. siRNA delivery with chitosan: Influence of chitosan molecular weight, degree of deacetylation, and amine to phosphate ratio on in vitro silencing efficiency, hemocompatibility, biodistribution, and in vivo efficacy. *Biomacromolecules* **2018**, *19*, 112−131.
(13) Ewert, K. K.; Zidovska, A.; Ahmad, A.; Bouxsein, N. F.; Evans, H. M.; McAllister, C. S.; Samuel, C. E.; Safinya, C. R. Cationic Liposome−Nucleic Acid Complexes for Gene Delivery and Silencing: Pathways and Mechanisms for Plasmid DNA and siRNA. In *Nucleic Acid Transfection*; Bielke, W.; Erbacher, C., Eds; Springer Berlin Heidelberg: Berlin, Heidelberg, 2010, pp. 191−226.
(14) Yoshioka, H.; Nonaka, K.-i.; Fukuda, K.; Kazama, S. Chitosan-derived polymer-surfactants and their micellar properties. *Biosci., Biotechnol., Biochem.* **1995**, *59*, 1901−1904.
(15) Guan, X.; Guo, Z.; Lin, L.; Chen, J.; Tian, H.; Chen, X. Ultrasensitive pH Triggered Charge/Size Dual-Rebound Gene Delivery System. *Nano Lett.* **2016**, *16*, 6823−6831.
(16) Sun, Q.; Zhou, Z.; Qiu, N.; Shen, Y. Rational Design of Cancer Nanomedicine: Nanoproperty Integration and Synchronization. *Adv. Mater.* **2017**, *29*, 1606628.
(17) Ogris, M.; Brunner, S.; Schüller, S.; Kircheis, R.; Wagner, E. PEGylated DNA/transferrin−PEI complexes: reduced interaction with blood components, extended circulation in blood and potential for systemic gene delivery. *Gene Ther.* **1999**, *6*, 595−605.
(18) Chen, J.; Dong, X.; Feng, T.; Lin, L.; Guo, Z.; Xia, J.; Tian, H.; Chen, X. Charge-conversional zwitterionic copolymer as pH-sensitive shielding system for effective tumor treatment. *Acta Biomater.* **2015**, *26*, 45−53.
(19) Tian, H.; Guo, Z.; Lin, L.; Jiao, Z.; Chen, J.; Gao, S.; Zhu, X.; Chen, X. pH-responsive zwitterionic copolypeptides as charge conversional shielding system for gene carriers. *J. Controlled Release* **2014**, *174*, 117−125.
(20) Chen, J.; Guo, Z.; Tian, H.; Chen, X. Production and clinical development of nanoparticles for gene delivery. *Mol. Ther.- - Methods Clin. Dev.* **2016**, *3*, 16023.
(21) Sogias, I. A.; Khutoryanskiy, V. V.; Williams, A. C. Exploring the Factors Affecting the Solubility of Chitosan in Water. *Macromol. Chem. Phys.* **2010**, *211*, 426−433.
(22) Jia, H.-R.; Jiang, Y.-W.; Zhu, Y.-X.; Li, Y.-H.; Wang, H.-Y.; Han, X.; Yu, Z.-W.; Gu, N.; Liu, P.; Chen, Z.; Wu, F. G. Plasma membrane activatable polymeric nanotheranostics with self-enhanced light-triggered photosensitizer cellular influx for photodynamic cancer therapy. *J. Controlled Release* **2017**, *255*, 231−241.
(23) Lin, F.; Jia, H.-R.; Wu, F.-G. Glycol chitosan: A water-soluble polymer for cell imaging and drug delivery. *Molecules* **2019**, *24*, 4371.
(24) Lin, W. J.; Hsu, W. Y. Pegylation effect of chitosan based polyplex on DNA transfection. *Carbohydr. Polym.* **2015**, *120*, 7−14.
(25) Zhao, J.; Li, J.; Jiang, Z.; Tong, R.; Duan, X.; Bai, L.; Shi, J. Chitosan, N,N,N-trimethyl chitosan (TMC) and 2-hydroxypropyl-trimethyl ammonium chloride chitosan (HTCC): The potential immune adjuvants and nano carriers. *Int. J. Biol. Macromol.* **2020**, *154*, 339−348.
(26) Zhao, X.; Yin, L.; Ding, J.; Tang, C.; Gu, S.; Yin, C.; Mao, Y. Thiolated trimethyl chitosan nanocomplexes as gene carriers with high in vitro and in vivo transfection efficiency. *J. Controlled Release* **2010**, *144*, 46−54.
(27) Tang, S.; Huang, Z.; Zhang, H.; Wang, Y.; Hu, Q.; Jiang, H. Design and formulation of trimethylated chitosan-graft-poly(ϵ-caprolactone) nanoparticles used for gene delivery. *Carbohydr. Polym.* **2014**, *101*, 104−112.
(28) Zhai, X.; Sun, P.; Luo, Y.; Ma, C.; Xu, J.; Liu, W. Guanidinylation: A simple way to fabricate cell penetrating peptide analogue-modified chitosan vector for enhanced gene delivery. *J. Appl. Polym. Sci.* **2011**, *121*, 3569−3578.
(29) Layek, B.; Singh, J. Amino acid grafted chitosan for high performance gene delivery: comparison of amino acid hydrophobicity on vector and polyplex characteristics. *Biomacromolecules* **2013**, *14*, 485−494.
(30) Wong, K.; Sun, G.; Zhang, X.; Dai, H.; Liu, Y.; He, C.; Leong, K. W. PEI-g-chitosan, a Novel Gene Delivery System with Transfection Efficiency Comparable to Polyethylenimine in Vitro

and after Liver Administration in Vivo. *Bioconjugate Chem.* **2006**, *17*, 152−158.
(31) Liu, X.; Mo, Y.; Liu, X.; Guo, R.; Zhang, Y.; Xue, W.; Zhang, Y.; Wang, C.; Ramakrishna, S. Synthesis, characterisation and preliminary investigation of the haemocompatibility of polyethyleneimine-grafted carboxymethyl chitosan for gene delivery. *Mater. Sci. Eng., C* **2016**, *62*, 173−182.
(32) Germershaus, O.; Mao, S.; Sitterberg, J.; Bakowsky, U.; Kissel, T. Gene delivery using chitosan, trimethyl chitosan or polyethylenglycol-graft-trimethyl chitosan block copolymers: establishment of structure-activity relationships in vitro. *J. Controlled Release* **2008**, *125*, 145−154.
(33) Jiang, G.-B.; Quan, D.; Liao, K.; Wang, H. Novel Polymer Micelles Prepared from Chitosan Grafted Hydrophobic Palmitoyl Groups for Drug Delivery. *Mol. Pharmaceutics* **2006**, *3*, 152−160.
(34) Thotakura, N.; Dadarwal, M.; Kumar, P.; Sharma, G.; Guru, S. K.; Bhushan, S.; Raza, K.; Katare, O. P. Chitosan-Stearic Acid Based Polymeric Micelles for the Effective Delivery of Tamoxifen: Cytotoxic and Pharmacokinetic Evaluation. *AAPS PharmSciTech* **2017**, *18*, 759−768.
(35) Meng, T.; Wu, J.; Yi, H.; Liu, J.; Lu, B.; Yuan, M.; Huang, X.; Yuan, H.; Hu, F. A spermine conjugated stearic acid-g-chitosan oligosaccharide polymer with different types of amino groups for efficient p53 gene therapy. *Colloids Surf., B* **2016**, *145*, 695−705.
(36) Du, Y.-Z.; Lu, P.; Zhou, J.-P.; Yuan, H.; Hu, F.-Q. Stearic acid grafted chitosan oligosaccharide micelle as a promising vector for gene delivery system: Factors affecting the complexation. *Int. J. Pharm.* **2010**, *391*, 260−266.
(37) Layek, B.; Singh, J. Caproic acid grafted chitosan cationic nanocomplexes for enhanced gene delivery: effect of degree of substitution. *Int. J. Pharm.* **2013**, *447*, 182−191.
(38) Sharma, D.; Singh, J. Synthesis and Characterization of Fatty Acid Grafted Chitosan Polymer and Their Nanomicelles for Nonviral Gene Delivery Applications. *Bioconjugate Chem.* **2017**, *28*, 2772−2783.
(39) Kim, Y. H.; Gihm, S. H.; Park, C. R.; Lee, K. Y.; Kim, T. W.; Kwon, I. C.; Chung, H.; Jeong, S. Y. Structural Characteristics of Size-Controlled Self-Aggregates of Deoxycholic Acid-Modified Chitosan and Their Application as a DNA Delivery Carrier. *Bioconjugate Chem.* **2001**, *12*, 932−938.
(40) Chen, H.; Cui, S.; Zhao, Y.; Wang, B.; Zhang, S.; Chen, H.; Peng, X. O-Alkylation of Chitosan for Gene Delivery by Using Ionic Liquid in an in- situ Reactor. *Engineering* **2012**, *04*, 114−117.
(41) Xiong, W.; Zhao, G. D.; Yin, X.; Linghu, K. G.; Chu, J. M. T.; Wong, G. T. C.; Li, H.; Yu, H.; Wang, Y. T. Brij-grafted-chitosan copolymers with function of P-glycoprotein modulation: Synthesis, characterization and in vitro investigations. *Carbohydr. Polym.* **2019**, *204*, 89−96.
(42) Layek, B.; Haldar, M. K.; Sharma, G.; Lipp, L.; Mallik, S.; Singh, J. Hexanoic acid and polyethylene glycol double grafted amphiphilic chitosan for enhanced gene delivery: influence of hydrophobic and hydrophilic substitution degree. *Mol. Pharmaceutics* **2014**, *11*, 982−994.
(43) Sang Yoo, H.; Eun Lee, J.; Chung, H.; Chan Kwon, I.; Young Jeong, S. Self-assembled nanoparticles containing hydrophobically modified glycol chitosan for gene delivery. *J. Controlled Release* **2005**, *103*, 235−243.
(44) Kwon, S.; Park, J. H.; Chung, H.; Kwon, I. C.; Jeong, S. Y.; Kim, I.-S. Physicochemical Characteristics of Self-Assembled Nanoparticles Based on Glycol Chitosan Bearing 5*β*-Cholanic Acid. *Langmuir* **2003**, *19*, 10188−10193.
(45) Kalliola, S.; Repo, E.; Srivastava, V.; Zhao, F.; Heiskanen, J. P.; Sirviö, J. A.; Liimatainen, H.; Sillanpää, M. Carboxymethyl Chitosan and Its Hydrophobically Modified Derivative as pH-Switchable Emulsifiers. *Langmuir* **2018**, *34*, 2800−2806.
(46) Tezgel, O.; Szarpak-Jankowska, A.; Arnould, A.; Auzely-Velty, R.; Texier, I. Chitosan-lipid nanoparticles (CS-LNPs): Application to siRNA delivery. *J. Colloid Interface Sci.* **2018**, *510*, 45−56.
(47) Uchegbu, I. F.; Sadiq, L.; Pardakhty, A.; El-Hammadi, M.; Gray, A. I.; Tetley, L.; Wang, W.; Zinselmeyer, B. H.; Schatzlein, A. G. Gene transfer with three amphiphilic glycol chitosans–the degree of polymerisation is the main controller of transfection efficiency. *J. Drug Targeting* **2004**, *12*, 527−539.
(48) Bhattacharya, S.; Bajaj, A. Advances in gene delivery through molecular design of cationic lipids. *Chem. Commun.* **2009**, *31*, 4632−4656.
(49) Yingyongnarongkul, B. E.; Radchatawedchakoon, W.; Krajarng, A.; Watanapokasin, R.; Suksamrarn, A. High transfection efficiency and low toxicity cationic lipids with aminoglycerol−diamine conjugate. *Bioorg. Med. Chem.* **2009**, *17*, 176−188.
(50) Khurana, A.; Allawadhi, P.; Khurana, I.; Allwadhi, S.; Weiskirchen, R.; Banothu, A. K.; Chhabra, D.; Joshi, K.; Bharani, K. K. Role of nanotechnology behind the success of mRNA vaccines for COVID-19. *Nano Today* **2021**, *38*, 101142.
(51) Bouraoui, A.; Ghanem, R.; Berchel, M.; Deschamps, L.; Vié, V.; Paboeuf, G.; Le Gall, T.; Montier, T.; Jaffrès, P.-A. Branched lipid chains to prepare cationic amphiphiles producing hexagonal aggregates: supramolecular behavior and application to gene delivery. *Org. Biomol. Chem.* **2020**, *18*, 337−345.
(52) Dominska, M.; Dykxhoorn, D. M. Breaking down the barriers: siRNA delivery and endosome escape. *J. Cell Sci.* **2010**, *123*, 1183.
(53) Felgner, J. H.; Kumar, R.; Sridhar, C. N.; Wheeler, C. J.; Tsai, Y. J.; Border, R.; Ramsey, P.; Martin, M.; Felgner, P. L. Enhanced gene delivery and mechanism studies with a novel series of cationic lipid formulations. *J. Biol. Chem.* **1994**, *269*, 2550−2561.
(54) Mönkkönen, J.; Urtti, A. Lipid fusion in oligonucleotide and gene delivery with cationic lipids. *Adv. Drug Delivery Rev.* **1998**, *34*, 37−49.
(55) Li, H.; Zhang, Z.; Bao, X.; Xu, G.; Yao, P. Fatty acid and quaternary ammonium modified chitosan nanoparticles for insulin delivery. *Colloids Surf., B* **2018**, *170*, 136−143.
(56) Cheng, Y.; Cai, H.; Yin, B.; Yao, P. Cholic acid modified N-(2-hydroxy)-propyl-3-trimethylammonium chitosan chloride for superoxide dismutase delivery. *Int. J. Pharm.* **2013**, *454*, 425−434.
(57) Li, G. F.; Wang, J. C.; Feng, X. M.; Liu, Z. D.; Jiang, C. Y.; Yang, J. D. Preparation and testing of quaternized chitosan nanoparticles as gene delivery vehicles. *Appl. Biochem. Biotechnol.* **2015**, *175*, 3244−3257.
(58) Thanou, M.; Florea, B. I.; Geldof, M.; Junginger, H. E.; Borchard, G. Quaternized chitosan oligomers as novel gene delivery vectors in epithelial cell lines. *Biomaterials* **2002**, *23*, 153−159.
(59) Silva, D. S.; M dos Santos, D.; Almeida, A.; Marchiori, L.; Campana-Filho, S. P.; Ribeiro, S. J.; Sarmento, B. N-(2-Hydroxy)-propyl-3-trimethylammonium, O-Mysristoyl Chitosan Enhances the Solubility and Intestinal Permeability of Anticancer Curcumin. *Pharmaceutics* **2018**, DOI: 10.3390/pharmaceutics10040245.
(60) Silva, D. S.; Facchinatto, W. M.; Dos Santos, D. M.; Boni, F. I.; Valdes, T. A.; Leitao, A.; Gremiao, M. P. D.; Colnago, L. A.; Campana-Filho, S. P.; Ribeiro, S. J. L. N-(2-hydroxy)-propyl-3-trimethylammonium, O-palmitoyl chitosan: Synthesis, physicochemical and biological properties. *Int. J. Biol. Macromol.* **2021**, *178*, 558−568.
(61) dos Santos, D. M.; Bukzem Ade, L.; Campana-Filho, S. P. Response surface methodology applied to the study of the microwave-assisted synthesis of quaternized chitosan. *Carbohydr. Polym.* **2016**, *138*, 317−326.
(62) Eaton, P.; Quaresma, P.; Soares, C.; Neves, C.; De Almeida, M.; Pereira, E.; West, P. A direct comparison of experimental methods to measure dimensions of synthetic nanoparticles. *Ultramicroscopy* **2017**, *182*, 179−190.
(63) Fissan, H.; Ristig, S.; Kaminski, H.; Asbach, C.; Epple, M. Comparison of different characterization methods for nanoparticle dispersions before and after aerosolization. *Anal. Methods* **2014**, *6*, 7324−7334.
(64) Gan, Q.; Wang, T.; Cochrane, C.; McCarron, P. Modulation of surface charge, particle size and morphological properties of

https://doi.org/10.1021/acsomega.1c06101
ACS Omega 2022, 7, 10056−10068

chitosan−TPP nanoparticles intended for gene delivery. *Colloids Surf., B* **2005**, *44*, 65−73.
(65) Desai, M. P.; Labhasetwar, V.; Amidon, G. L.; Levy, R. J. Gastrointestinal Uptake of Biodegradable Microparticles: Effect of Particle Size. *Pharm. Res.* **1996**, *13*, 1838−1845.
(66) He, C.; Hu, Y.; Yin, L.; Tang, C.; Yin, C. Effects of particle size and surface charge on cellular uptake and biodistribution of polymeric nanoparticles. *Biomaterials* **2010**, *31*, 3657−3666.
(67) Lee, J. H.; Lim, Y.-b.; Choi, J. S.; Lee, Y.; Kim, T.-i.; Kim, H. J.; Yoon, J. K.; Kim, K.; Park, J. S. Polyplexes Assembled with Internally Quaternized PAMAM-OH Dendrimer and Plasmid DNA Have a Neutral Surface and Gene Delivery Potency. *Bioconjugate Chem.* **2003**, *14*, 1214−1221.
(68) Blessing, T.; Remy, J.-S.; Behr, J.-P. Monomolecular collapse of plasmid DNA into stable virus-like particles. *Proc. Natl. Acad. Sci.* **1998**, *95*, 1427−1431.
(69) Kim, S. I.; Kim, H. J.; Lee, H.-J.; Lee, K.; Hong, D.; Lim, H.; Cho, K.; Jung, N.; Yi, Y. W. Application of a non-hazardous vital dye for cell counting with automated cell counters. *Anal. Biochem.* **2016**, *492*, 8−12.
(70) Tominaga, H.; Ishiyama, M.; Ohseto, F.; Sasamoto, K.; Hamamoto, T.; Suzuki, K.; Watanabe, M. A water-soluble tetrazolium salt useful for colorimetric cell viability assay. *Anal. Commun.* **1999**, *36*, 47−50.
(71) Strober, W. Trypan blue exclusion test of cell viability. *Curr. Protoc. Immunol.* **1997**, *21*, A−3B.
(72) Chatelet, C.; Damour, O.; Domard, A. Influence of the degree of acetylation on some biological properties of chitosan films. *Biomaterials* **2001**, *22*, 261−268.
(73) Dhiman, H. K.; Ray, A. R.; Panda, A. K. Characterization and evaluation of chitosan matrix for in vitro growth of MCF-7 breast cancer cell lines. *Biomaterials* **2004**, *25*, 5147−5154.
(74) Xiao, B.; Wan, Y.; Wang, X.; Zha, Q.; Liu, H.; Qiu, Z.; Zhang, S. Synthesis and characterization of N-(2-hydroxy)propyl-3-trimethyl ammonium chitosan chloride for potential application in gene delivery. *Colloids Surf., B* **2012**, *91*, 168−174.
(75) Layek, B.; Singh, J. Cell penetrating peptide conjugated polymeric micelles as a high performance versatile nonviral gene carrier. *Biomacromolecules* **2013**, *14*, 4071−4081.
(76) Wang, B.; He, C.; Tang, C.; Yin, C. Effects of hydrophobic and hydrophilic modifications on gene delivery of amphiphilic chitosan based nanocarriers. *Biomaterials* **2011**, *32*, 4630−4638.
(77) Wang, J.; Jiang, J. Z.; Chen, W.; Bai, Z. W. Data of $^{1}H/^{13}C$ NMR spectra and degree of substitution for chitosan alkyl urea. *Data in Brief* **2016**, *7*, 1228−1236.
(78) Kasaai, M. R. Determination of the degree of N-acetylation for chitin and chitosan by various NMR spectroscopy techniques: A review. *Carbohydr. Polym.* **2010**, *79*, 801−810.

https://doi.org/10.1021/acsomega.1c06101
ACS Omega 2022, 7, 10056−10068